EUROPEAN ORGANIZATION FOR NUCLEAR RESEARCH

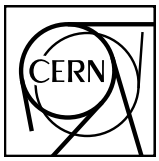

ALICE-PUBLIC-2015-001

Supplemental figures: Measurement of prompt D-meson production in p–Pb collisions at $\sqrt{s_{\rm NN}} = 5.02$ TeV

ALICE Collaboration*

Abstract

This note provides supplemental figures for the analysis on the "Measurement of prompt D-meson production in p–Pb collisions at $\sqrt{s_{\rm NN}} = 5.02$ TeV" published on PRL 113, 232301 (2014), arXiv:1405.3452.

*The author list is given in PRL 113, 232301 (2014)

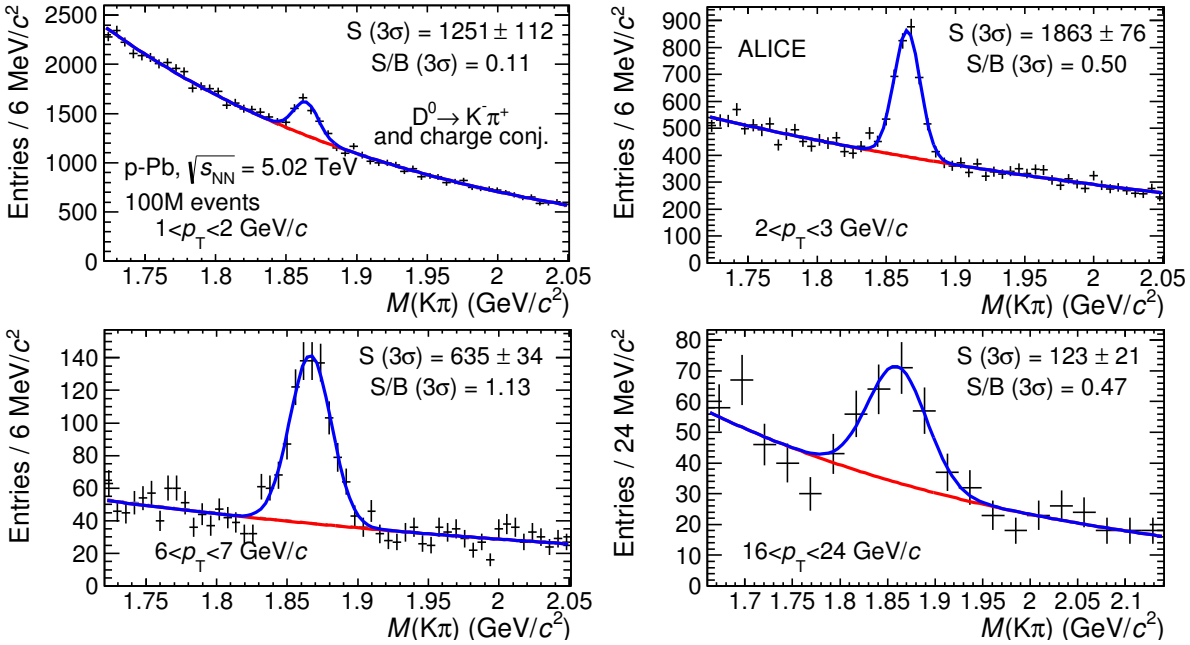

Fig. 1: Invariant mass distributions of D^0 candidates and charge conjugates in four selected p_T intervals considered for the analysis. The topological and kinematical selections applied to obtain these distributions are described in the paper. The fit functions showed in the figure consist of a sum of a Gaussian and an exponential to describe the signal and the background respectively. The values of the signal (S) and background counts (B) integrated in $\pm 3\sigma$ region around the centroid of the Gaussian are reported.

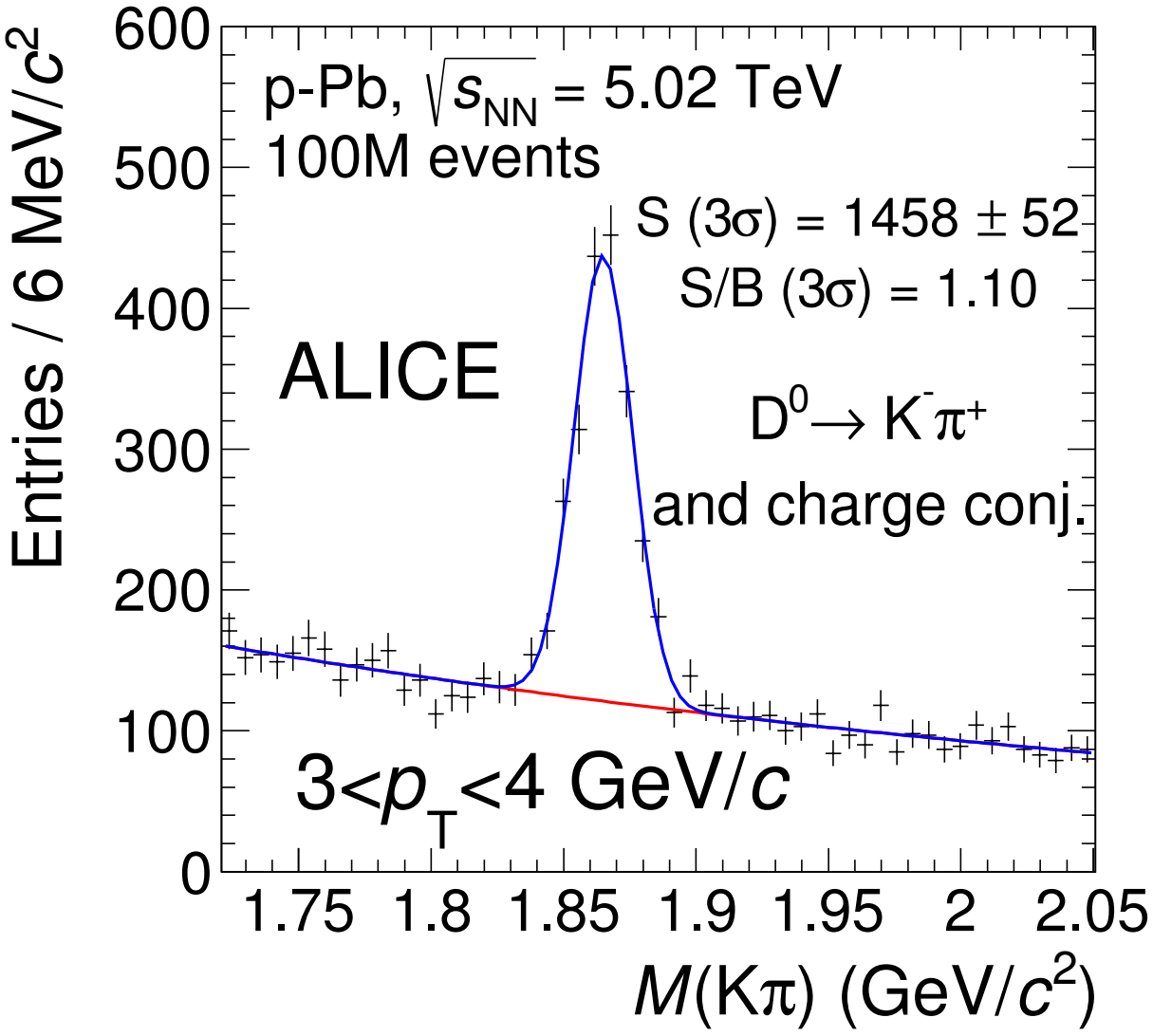

Fig. 2: Invariant mass distributions of D^0 candidates and charge conjugates in the momentum interval $3 < p_T < 4$ GeV/c.The values of the signal (S) and background counts (B) integrated in $\pm 3\sigma$ region around the centroid of the Gaussian are reported.

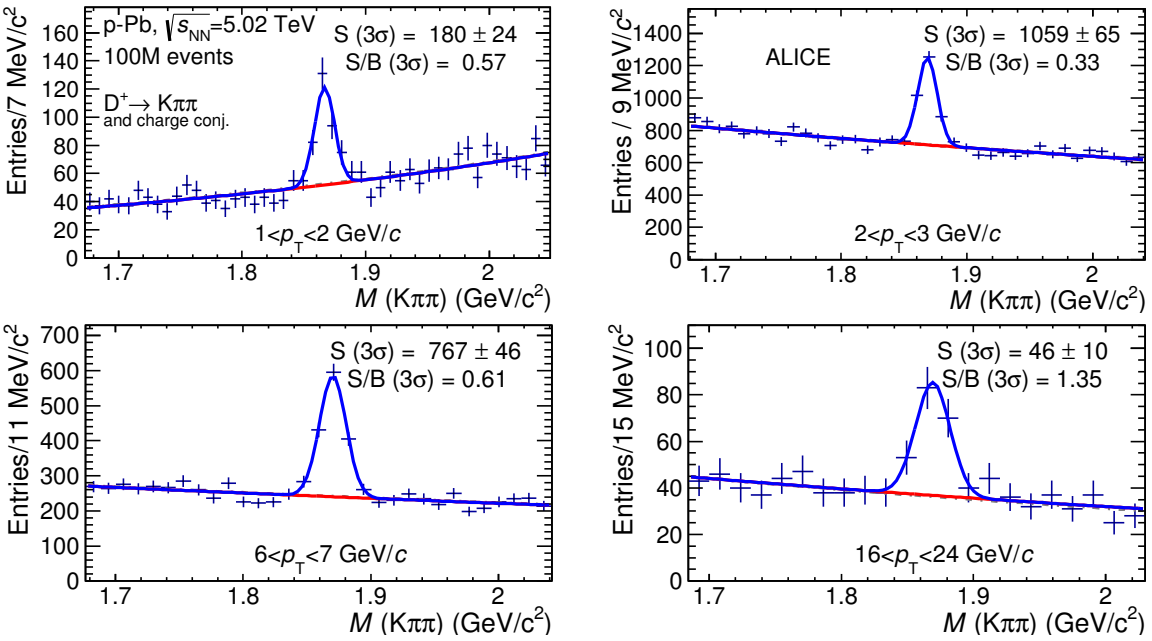

Fig. 3: Invariant mass distributions of D^+ candidates and charge conjugates in four selected p_T intervals considered for the analysis. The topological and kinematical selections applied to obtain these distributions are described in the paper. The fit functions showed in the figure consist of a sum of a Gaussian and an exponential to describe the signal and the background respectively. The values of the signal (S) and background counts (B) integrated in $\pm 3\sigma$ region around the centroid of the Gaussian are reported.

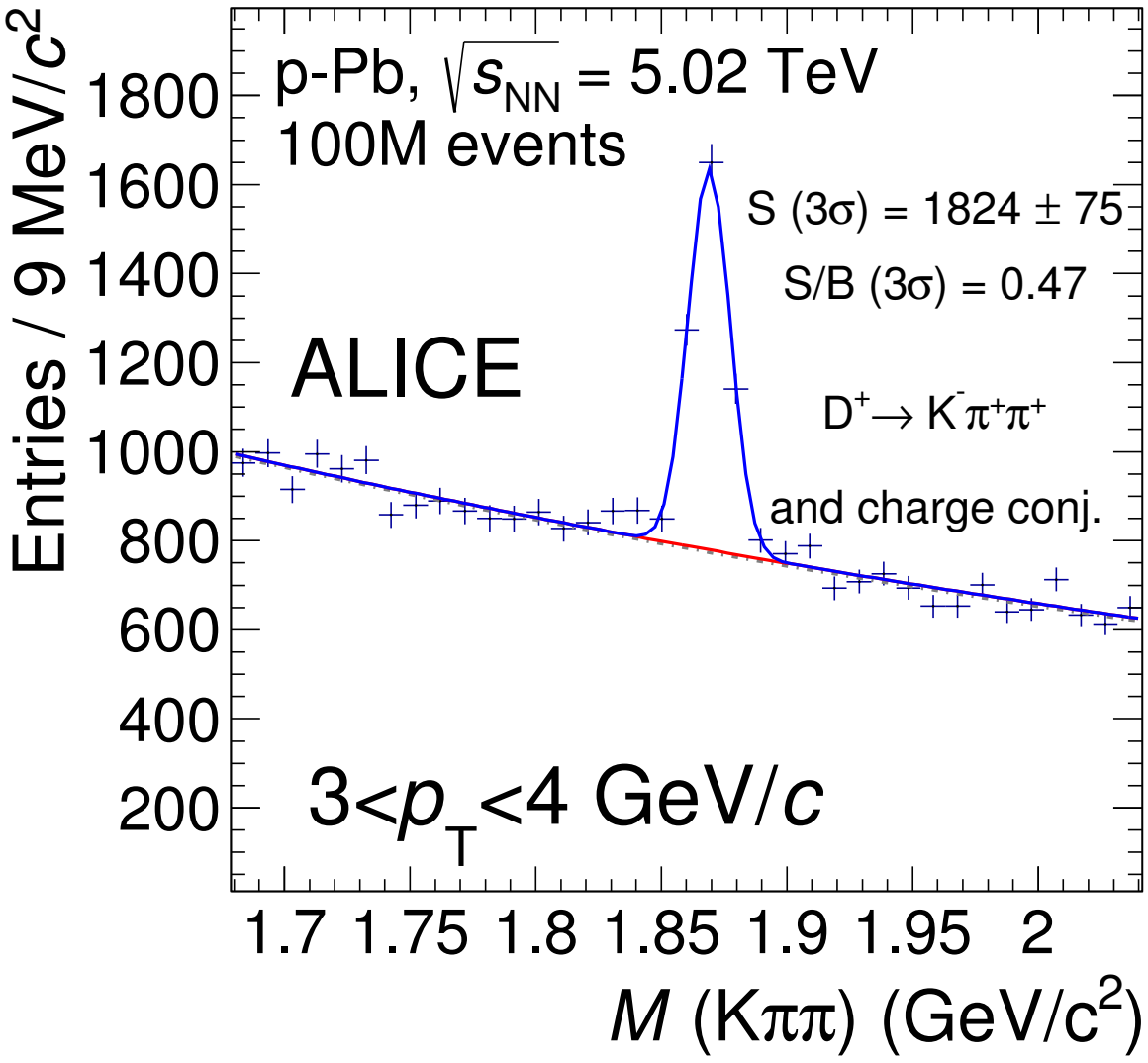

Fig. 4: Invariant mass distributions of D^+ candidates and charge conjugates in the momentum interval $3 < p_T < 4$ GeV/c.The values of the signal (S) and background counts (B) integrated in $\pm 3\sigma$ region around the centroid of the Gaussian are reported.

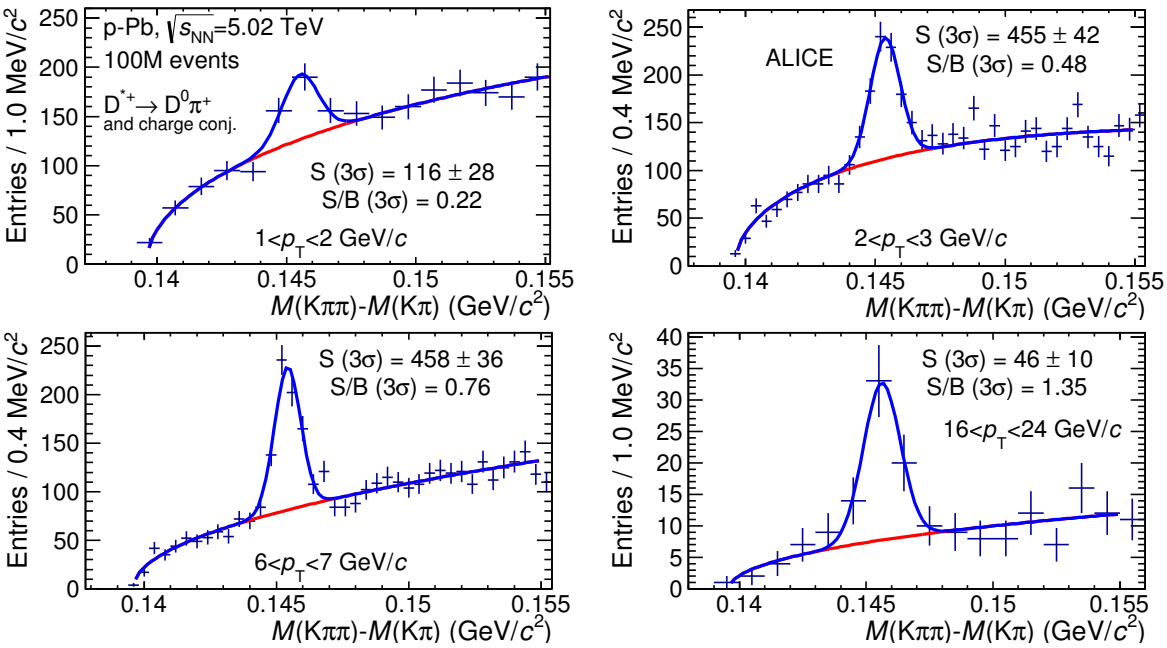

Fig. 5: Mass difference distributions of D^{*+} candidates and charge conjugates in four selected p_T intervals considered for the analysis. The topological and kinematical selections applied to obtain these distributions are described in the paper. The fit functions showed in the figure consist of a sum of Gaussian and a threshold function ($a\sqrt{\Delta M - M_\pi} \cdot e^{b(\Delta M - M_\pi)}$, where M_π is the pion mass and a and b are free parameters) to describe the signal and the background respectively. The values of the signal (S) and background counts (B) integrated in $\pm 3\sigma$ region around the centroid of the Gaussian are reported.

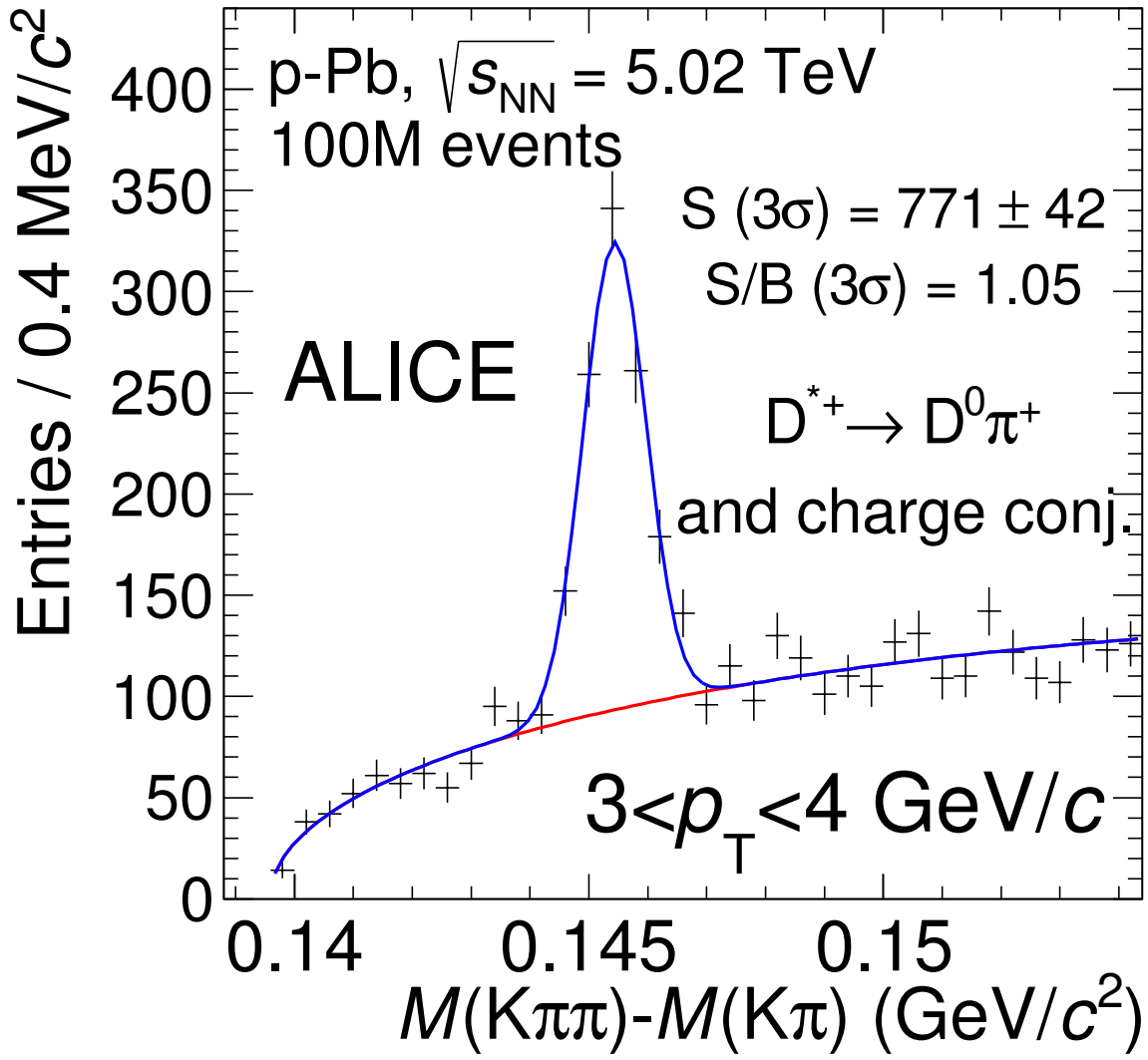

Fig. 6: Invariant mass distributions of D^{*+} candidates and charge conjugates in the momentum interval $3 < p_T < 4$ GeV/c.The values of the signal (S) and background counts (B) integrated in $\pm 3\sigma$ region around the centroid of the Gaussian are reported.

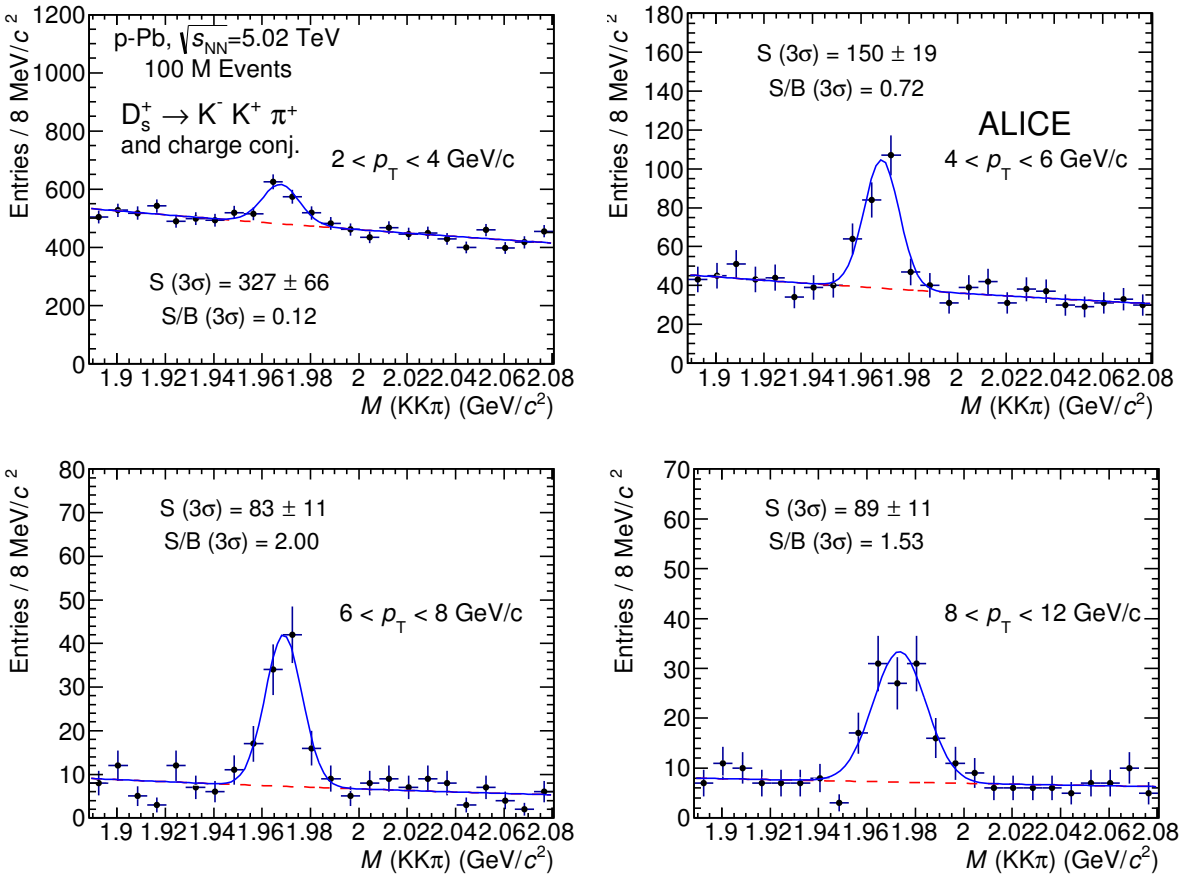

Fig. 7: Invariant mass distributions of D_s^+ candidates and charge conjugates in the 4 p_T intervals considered for the analysis. The topological and kinematical selections applied to obtain these distributions are described in the paper. The fit functions showed in the figure consist of a sum of a Gaussian and an exponential to describe the signal and the background respectively. The values of the signal (S) and background counts (B) integrated in $\pm 3\sigma$ region around the centroid of the Gaussian are reported.

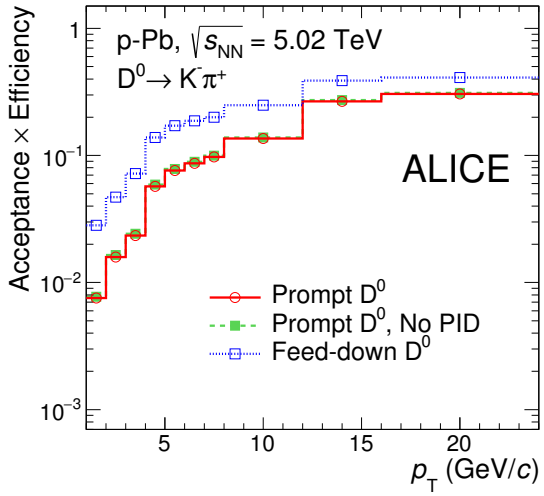

(a) D^0 meson

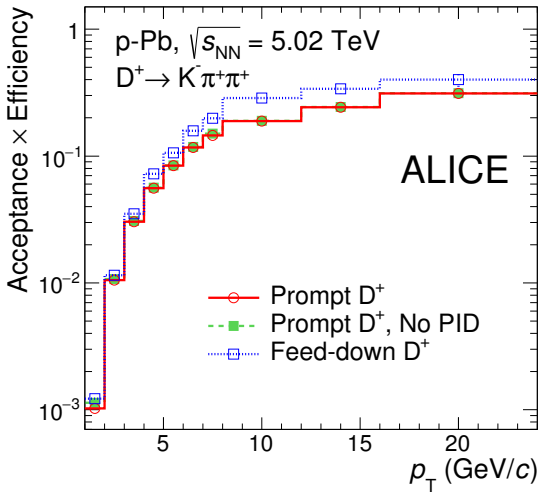

(b) D^+ meson

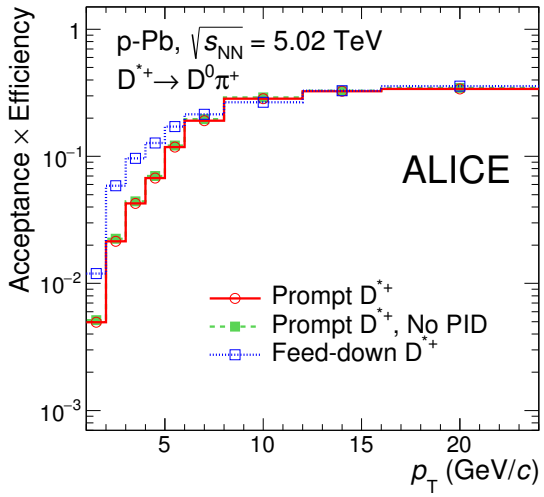

(c) D^{*+} meson

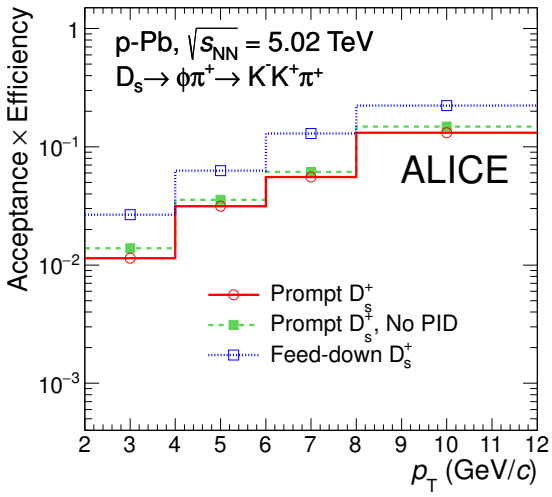

(d) D_s^+ meson

Fig. 8: Acceptance × efficiency corrections for prompt D^0, D^+, D^{*+} and D_s^+ mesons (red empty circles) and for feed-down D^0, D^+, D^{*+} and D_s^+ from B hadrons decays (blue empty squares) as a function of p_T. The efficiency without particle identification (filled green squares) is also shown for comparison.

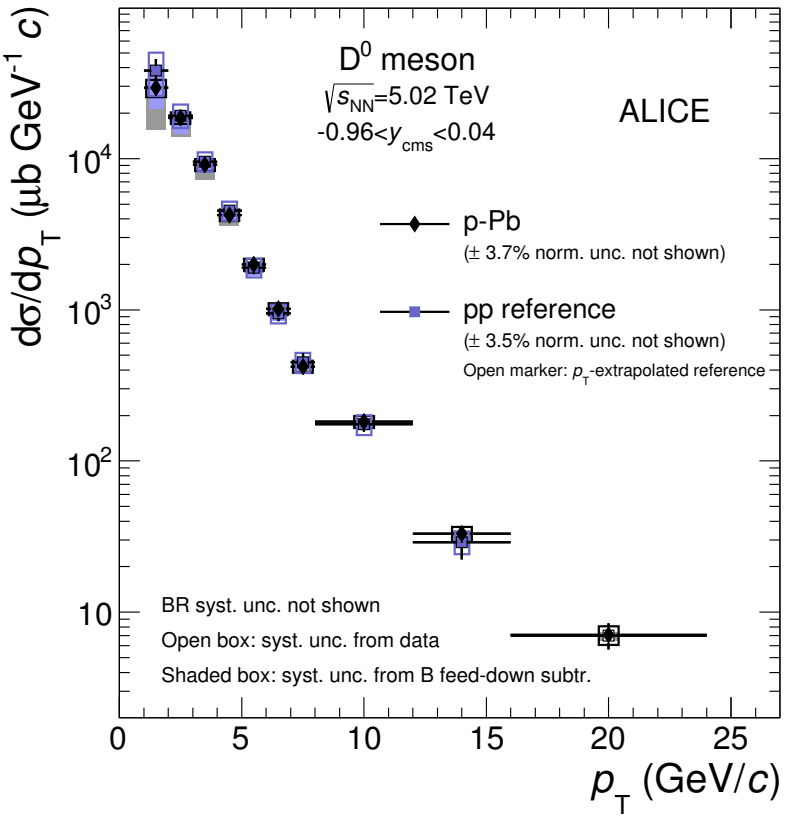

Fig. 9: p_{T}-differential production cross section of prompt D^0 mesons in p–Pb minimum-bias collisions at $\sqrt{s_{\mathrm{NN}}} = 5.02$ TeV compared with a pp rescaled reference af the same center-of-mass $A\mathrm{d}\sigma/\mathrm{d}p_{\mathrm{T}}$, where A is the atomic mass number. Statistical uncertainties (bars) and systematic uncertainties from data analysis (empty boxes) and from feed-down subtraction (full boxes) are shown. Horizontal error bars reflect the bin widths, symbols are located at the center of the bin.

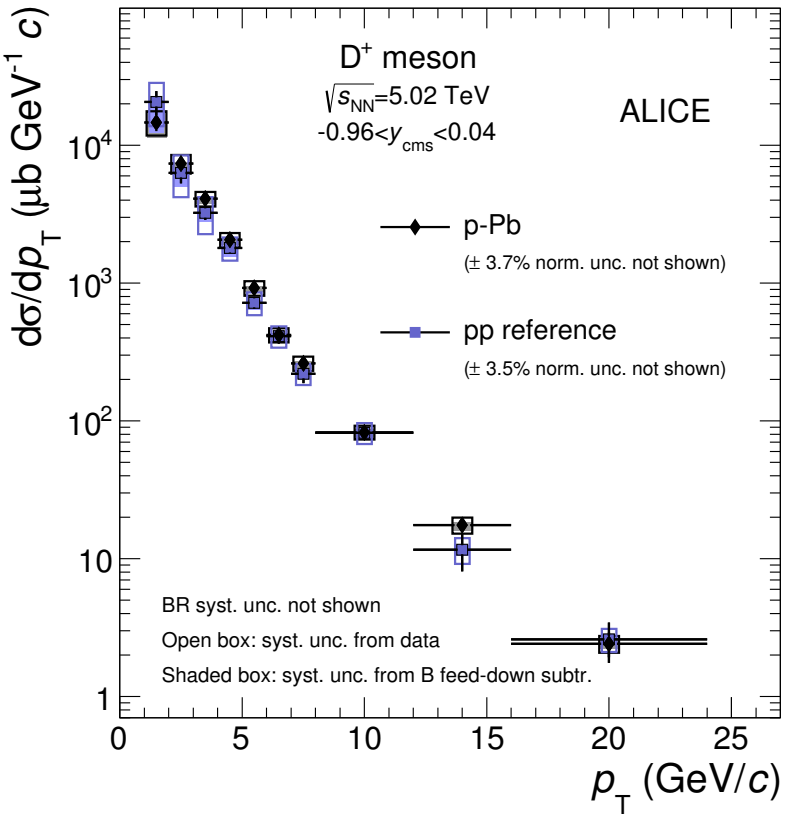

Fig. 10: p_{T}-differential production cross section of prompt D^{+} mesons in p–Pb minimum-bias collisions at $\sqrt{s_{\mathrm{NN}}} = 5.02$ TeV compared with a pp rescaled reference af the same center-of-mass $A\mathrm{d}\sigma/\mathrm{d}p_{\mathrm{T}}$, where A is the atomic mass number. Statistical uncertainties (bars) and systematic uncertainties from data analysis (empty boxes) and from feed-down subtraction (full boxes) are shown. Horizontal error bars reflect the bin widths, symbols are located at the center of the bin.

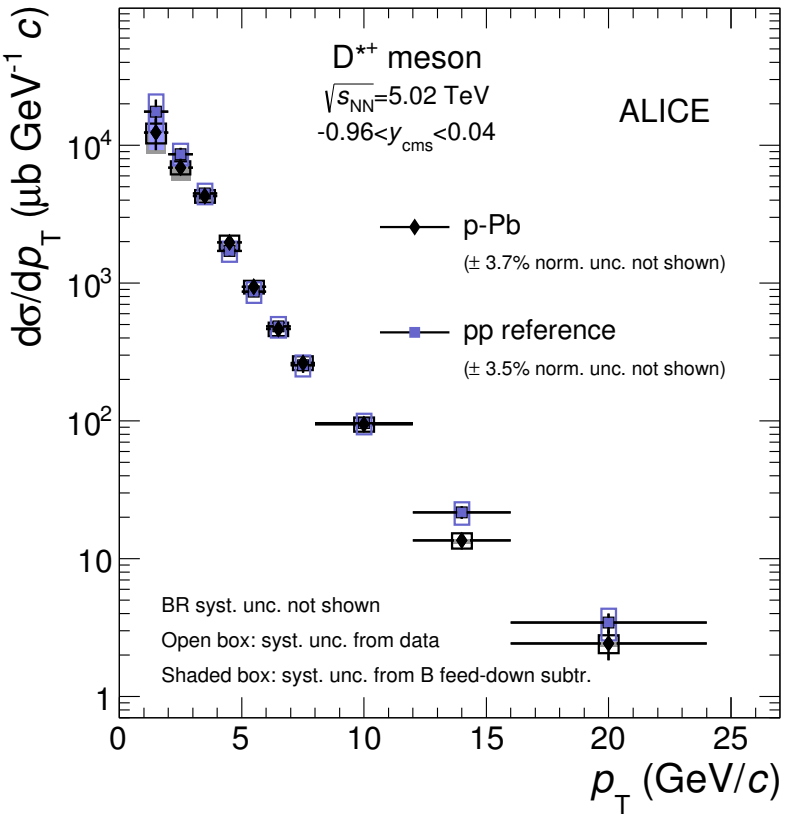

Fig. 11: p_{T}-differential production cross section of prompt D^{*+} mesons in p–Pb minimum-bias collisions at $\sqrt{s_{\mathrm{NN}}} = 5.02$ TeV compared with a pp rescaled reference af the same center-of-mass $A\mathrm{d}\sigma/\mathrm{d}p_{\mathrm{T}}$, where A is the atomic mass number. Statistical uncertainties (bars) and systematic uncertainties from data analysis (empty boxes) and from feed-down subtraction (full boxes) are shown. Horizontal error bars reflect the bin widths, symbols are located at the center of the bin.

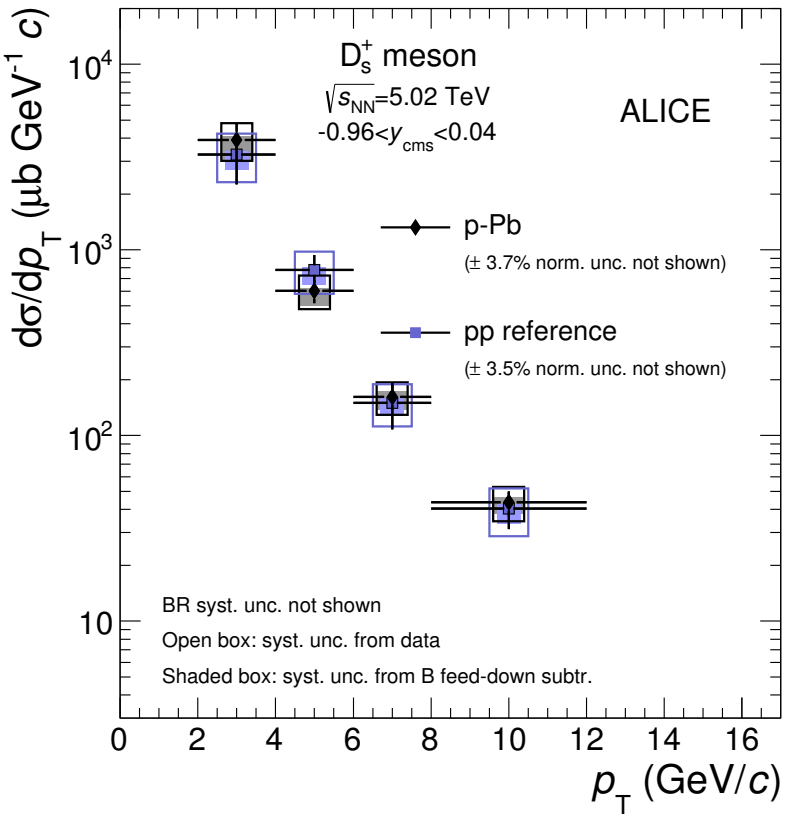

Fig. 12: p_{T}-differential production cross section of prompt $\mathrm{D_s^+}$ mesons in p–Pb minimum-bias collisions at $\sqrt{s_{\mathrm{NN}}} = 5.02$ TeV compared with a pp rescaled reference af the same center-of-mass $A\mathrm{d}\sigma/\mathrm{d}p_{\mathrm{T}}$, where A is the atomic mass number. Statistical uncertainties (bars) and systematic uncertainties from data analysis (empty boxes) and from feed-down subtraction (full boxes) are shown. Horizontal error bars reflect the bin widths, symbols are located at the center of the bin.